

Quasi-static macrostrain-based structural damage detection with distributed long-gauge fiber Bragg grating sensing

Zhenwei Zhou¹ , Chunfeng Wan¹, Da Fang¹, Liyu Xie², Hesheng Tang², Caiqian Yang³ , Youliang Ding¹ and Songtao Xue^{2,4}

Journal of Intelligent Material Systems and Structures

1–15

© The Author(s) 2020

Article reuse guidelines:

sagepub.com/journals-permissions

DOI: 10.1177/1045389X20942320

journals.sagepub.com/home/jim



Abstract

The distributed long-gauge fiber Bragg grating sensing technology has been studied and developed in recent years for structural health monitoring of civil engineering structures. Also, the corresponding damage identification method is one of the research hotspots and still needs to be enhanced. In this article, a novel damage detection method based on the distributed long-gauge fiber Bragg grating sensing technique is proposed to detect and localize damages. The method is based on the advanced complete ensemble empirical mode decomposition adaptive noise algorithm. Measured macrostrain responses from the long-gauge fiber Bragg grating sensors are decomposed into intrinsic mode functions, and the quasi-static macrostrains are extrapolated and extracted. A damage indicator is therefore proposed and built based on the quasi-static macrostrain time history. The effectiveness of the proposed damage detection approach was validated by numerical simulations of a cantilever beam. The robustness of the method was further verified by considering the noise pollution contained within the measured macrostrain. Experiments with a practical cantilever steel beam with different damage scenarios were also conducted and studied. Results proved that the proposed method could not only detect but also locate the damages accurately, and therefore has the promising potential for structural damage detection in civil engineering.

Keywords

damage detection, complete ensemble empirical mode decomposition adaptive noise method, quasi-static macrostrain, long-gauge fiber Bragg grating sensor

1. Introduction

In recent years, structural health monitoring (SHM) has been attracted wide attention, and many SHM systems have been built for civil engineering structures (Barke and Chiu, 2005; Ou and Li, 2010). The primary purpose of online monitoring is to detect damage in time, but local damage usually is embedded in the structural system and is hard to be observed, especially when it is rather slight. Thus, choosing sensitive and precise sensors, as well as sensitive damage indicators, is a critical issue in SHM.

In practical engineering applications, small defects usually could be detected from the variation of strains rather than that of displacements. Thus, strain gauge has the capacity to monitor local structural information and has been widely used in SHM for online monitoring (Sanayei and Onipede, 1991; Sanayei and

Saletnik, 1996). However, the traditional point strain gauge is too “local” to monitor the whole structures completely. Distributed long-gauge fiber Bragg grating (FBG) sensing technique aims to overcome this “local” problem, which measures the average strain within the

¹Southeast University, Key Laboratory of concrete and pre-stressed concrete structure of Ministry of Education, Nanjing, China

²Department of Disaster Mitigation for Structures, College of Civil Engineering, Tongji University, Shanghai, China

³College of Civil Engineering & Mechanics, Xiangtan University, Xiangtan, China

⁴Department of Architecture, Tohoku Institute of Technology, Sendai, Japan

Corresponding author:

Liyu Xie, Department of Disaster Mitigation for Structures, College of Civil Engineering, Tongji University, Shanghai 200092, China.
Email: liyuxie@tongji.edu.cn

gauge length and makes the real application of the strain-based method more widely (Li and Wu, 2007a). Thus, the distributed FBG sensing technique has been widely applied in SHM for different types of structures, such as railway tunnels (Ye et al., 2013), wind turbines (Arsenault et al., 2013), concrete bridges (Rodrigues et al., 2010). Many algorithms and methods have been proposed correspondingly to detect damages and evaluate the safety of structures. Li and Wu (2007b) developed a modal macrostrain vector (MMSV) to estimate damage in flexural structures. Hong et al. (2016) and Wu et al. (2017) proposed to use a macrostrain influence line for stiffness monitoring and damage identification of bridges under moving vehicle loads. Zhang et al. (2015) presented the frequency response function (FRF) of macrostrain to detect the local damage of a cantilever beam. Wu et al. (2016) extracted the quasi-static macrostrain to identify damage and assess the bearing capacity of a bridge. Other macrostrain-based indexes, such as the macrostrain ratio index (Kamrujjaman Serker et al., 2010), macrostrain-based energy index (Xu et al., 2011), were also received much attention. The distributed long-gauge sensing technique provides a promising measure for developing online SHM systems.

Measured data processing is an important and necessary part in the practical applications of SHM. The short-time Fourier Transform (Rippert et al., 2000) and wavelet analysis (Hou et al., 2000; Kim and Melhem, 2004) are important tools to decompose signals into components. However, they show lack of adaptability, especially when the field measured data are highly noisy and non-stationary. Empirical mode decomposition (EMD; Huang et al., 1998) and ensemble empirical mode decomposition (EEMD; Wu and Huang, 2009) were further proposed to decompose a measured response data into intrinsic mode functions (IMFs) for the non-stationary signals; they are also received much attention in structural damage detection. However, EMD often causes the mode-mixing problem while the EEMD brings new residue noise, which results in that the actual responses cannot be reconstructed accurately. Such disadvantages restrict the EMD-based and EEMD-based techniques severely. Recently, a complete ensemble empirical mode decomposition adaptive noise (CEEMDAN) method (Torres et al., 2011) was

proposed, which not only alleviates the mode mixing problem in EMD but also overcome the major drawback of residual noise in modes and spurious modes by EEMD. At present, the CEEMDAN-based methods are widely used in data forecasting (Ren et al., 2015; Zhang et al., 2017), de-noising (Abdelkader et al., 2018; Wang et al., 2018), and fault diagnosis (Bai et al., 2018), but few applied in damage detection for civil engineering structures.

In this article, a novel quasi-static macrostrain-based method is developed and proposed to detect local damages based on the distributed long-gauge FBG sensing system. The distributed long-gauge FBG sensors will be pasted on the surface of the structure to measure the macrostrain response of the structure. Quasi-static macrostrains are then extracted from the measured macrostrain responses based on the improved complete ensemble empirical mode decomposition adaptive noise (CEEMDAN) method. After that, a novel developed quasi-static macrostrain-based indicator is applied to detect the damages. Various numerical damage cases, with and without considering measurement noise, are selected to judge the efficiency of the proposed method for accurate damage detection. Experimental results further reveal that the proposed detection method and damage indicator can identify the small damages in a damaged structure rapidly and precisely.

2. Damage detection principle based on quasi-static macrostrain

2.1. Macrostrain time-history extraction

If a structure is deployed with a distributed long-gauge FBG sensor array, the distribution of the macrostrain along with the structure, that is, the average strain within the gauge length of each sensor, could then be obtained. As shown in Figure 1, an Euler beam suffers a small deformation, and the rotational displacements can be expressed as

$$\theta(x) \approx w' = y'(x) \quad (1)$$

where $w = y(x)$. θ and w are the rotation and the deflection, respectively.

Assuming that an Euler beam is divided into n elements, as shown in Figure 2, random loads are applied

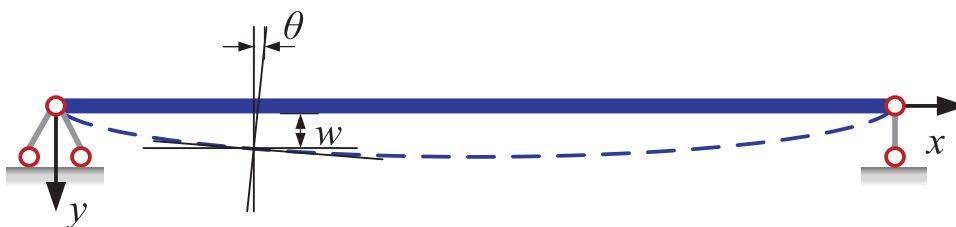


Figure 1. An Euler beam with a small deformation.

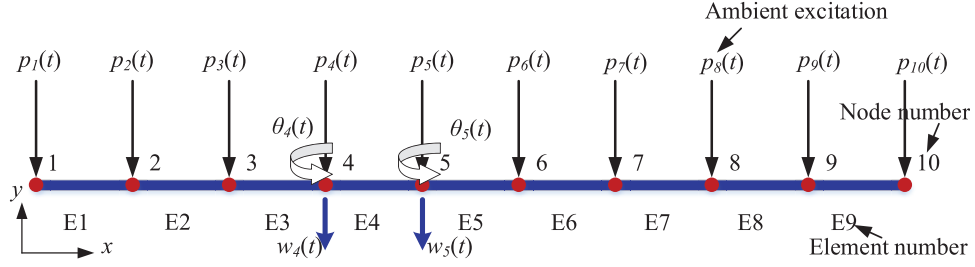


Figure 2. A beam under ambient excitations.

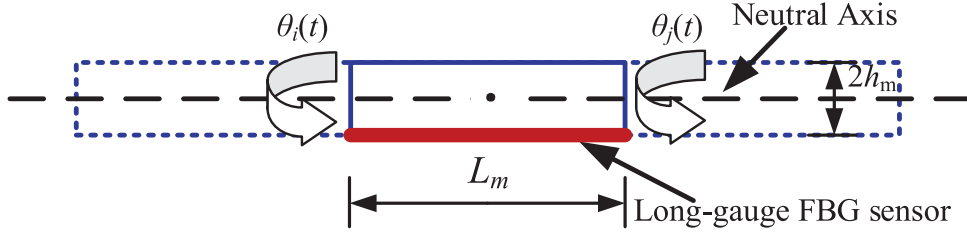


Figure 3. Schematic diagram of macrostrain calculation of an element.

to each node at the same time. According to the theory of material mechanics (Hibbeler, 2004), the relationship between the curvature $\kappa(x)$ and the moment $M(x)$ at any point on the beam can be represented as

$$\kappa(x) = \frac{M(x)}{EI} \quad (2)$$

where E and I are the elastic modulus and the moment of inertia, respectively.

Moreover, the relationship between curvature and deformation is given as

$$\kappa(x) = \frac{y''(x)}{(1 + y'(x))^3/2} \approx y''(x) \quad (3)$$

Thus, from the above analysis, the normal strain at any point can therefore be calculated by

$$\varepsilon(x) = \kappa(x)h_m = y''(x)h_m \quad (4)$$

where h_m is the distance between the sensor and the beam's neutral axis. m represents the m th long-gauge sensor. Figure 3 shows the m th long-gauge FBG sensor with gauge length L_m is pasted on the surface of the structure, and the macrostrain within this gauge length can be acquired from the rotational displacements at the adjacent nodes. It can be expressed as (Zhou et al., 2019)

$$\bar{\varepsilon}_m(x) = \frac{1}{L_m} \int_{x_i}^{x_j} y''(x)h_m dx = \frac{h_m}{L_m} (\theta(x_j) - \theta(x_i)) \quad (5)$$

where θ_i and θ_j are the rotational displacements of the m th element at i th and j th node, respectively.

2.2. The CEEMDAN method for dynamic and static strain response separation

The macrostrain response of the beam caused by ambient excitations is non-stationary and contains a variety of frequency components. It can be regarded as the superposition of long-period response trend and short-period disturbance, which are called static response component and dynamic response component, respectively. Here, the CEEMDAN method is introduced to separate the dynamic and quasi-static macrostrain components. First, we define an operator $E_j(\cdot)$, which can produce the j th mode of EMD for a given signal. Suppose $W_i(t)$ with $i = 1, 2, \dots, I$ are random white noise following the distribution of $N(0,1)$, which will be added to the original macrostrain response $\bar{\varepsilon}(t)$ as

$$\bar{\varepsilon}_i(t) = \bar{\varepsilon}(t) + W_i(t) \quad (6)$$

where $\bar{\varepsilon}_i(t)$ represent the synthesized macrostrain signal mixed with the white noise.

Since the $\bar{\varepsilon}_i(t)$ is composed of several different frequency components, it can be decomposed by EMD to obtain the first mode $IMF_1^i(t)$. The first mode $IMF_1(t)$ of CEEMDAN can be obtained as

$$IMF_1(t) = \frac{1}{I} \sum_{i=1}^I IMF_1^i(t) \quad (7)$$

At the first stage the first residue can be calculated as

$$r_1(t) = \bar{\varepsilon}(t) - IMF_1(t) \quad (8)$$

After that, if the remainder $r_1(t)$ is a monotonic function, the decomposition ends; if not, keep adding different white noise $W_i(t)$ to the $r_1(t)$. New synthetic

macrostrain, $r_1(t) + \alpha E_1(W_i(t)), i = 1, 2, \dots, I$, can be obtained until their first EMD mode and the second mode can be defined as

$$IMF_2(t) = \frac{1}{I} \sum_{i=1}^I E_1(r_1(t) + \alpha E_1(W_i(t))) \quad (9)$$

where α is the coefficient of signal-to-noise ratio. Similarly, the macrostrain can be decomposed until the last residue is indecomposable. Then, the original macrostrain time-history can be represented as

$$\bar{\varepsilon}(t) = \sum_{j=1}^J IMF_j(t) + r_j(t) \quad (10)$$

where j is the total number of the IMFs after the decomposition of CEEMDAN for the macrostrain response. $IMF_j(t)$ reflects the macrostrain response in a different frequency component, $r_j(t)$ is the residue and indecomposable. Thus, equation (10) makes the proposed decomposition complete and provides fairly accurate reconstruction.

2.3. The criteria for extracting quasi-static macrostrain

The IMFs reflect the components of different frequencies in the macrostrain and are ordered from high to low according to the frequency values. Set the first-order frequency as the threshold, the criteria for the dynamic and static strain separated from macrostrain response is as follows (Wu et al., 2016)

$$\begin{cases} \bar{\varepsilon}_d(t) = \sum_{i=1}^n c_i(t) & f(c_i(t)) \geq f_1 \\ \bar{\varepsilon}_s(t) = \sum_{i=1}^n c_i(t) + r_n(t) & f(c_i(t)) < f_1 \end{cases} \quad (11)$$

where $\bar{\varepsilon}_d$ and $\bar{\varepsilon}_s$ represent the dynamic and quasi-static macrostrain response extracted from the long-gauge macrostrain response, respectively. $f(c_i(t))$ and f_1 represent the frequency of the i th IMF and the first-order frequency of the structures, respectively. n is the total number of IMFs and $r_n(t)$ is the remainder. The main procedure of extracting quasi-static macrostrain from the measurement strain response, as shown in Figure 4, can be summarized as follows:

Step 1: The structure is divided into N elements which are covered with the long-gauge FBG sensor. Then obtain the macrostrain response of each element from the long-gauge FBG sensors.

Step 2: The CEEMDAN technology is introduced to decompose the original macrostrain series into a

collection of IMFs with corresponding frequencies and the residue component.

Step 3: Determine the first-order frequency of the structure, and then select the quasi-static macrostrain components in the frequency domain. Thus, the quasi-static macrostrain components can be reconstructed in the time domain.

2.4. The quasi-static macrostrain-based damage indicator

For an effective damage detection method, the critical point is to choose an effective damage indicator which is sensitive to local damages but not to external noises and environmental conditions. In this study, a damage indicator based on the change of the quasi-static macrostrain is presented to detect the damages accurately. A type of macrostrain energy in time-domain, named as the quasi-static macrostrain energy, is proposed and given as

$$E_{sm} = \|\bar{\varepsilon}_{sm}(t)\|^2 = \int_{t_0}^{t_n} (\bar{\varepsilon}_{sm}(t))^2 dt \quad (m = 1, 2, \dots, N) \quad (12)$$

where t_0 and t_n are the start and the end time of the macrostrain sampling period, respectively. m is the series number of the calculated element, N is the total number of elements. Combining all the E_{sm} of the whole structure gives us a vector as

$$\mathbf{E}_s = [E_{s1}, E_{s2}, \dots, E_{sm}, \dots, E_{sN}] \quad (13)$$

It should be noted that the vector \mathbf{E}_s only emphasizes the quasi-static macrostrain energy for each element within a period of time. It could be different when it is subject to variable excitations, so that it can hardly provide useful information by simply comparing it before and after damage. Therefore, it is necessary to propose a normalized criterion which is suitable for indicating the different status of intact and damaged structures. A vector emphasizing the relative ratio of all components can therefore be further expressed as

$$\mathbf{RE}_s = [RE_{s1}, RE_{s2}, \dots, RE_{sm}, \dots, RE_{sN}] \quad (14)$$

where $RE_{sm} = E_{sm} / \sum_{i=1}^N E_{si}$, $m = 1, 2, \dots, N$ and $\sum_{m=1}^N RE_{sm} = 1$. As the damage locations are usually unknown for the damaged structure under ambient excitations, the macrostrain energy for element E_{sm} ($m = 1, 2, \dots, N$) of the structure before damage occurs is used to as a reference. An indicator for estimating the presence of damage in the element can then be defined and expressed as

$$\beta_m = \frac{[RE_{sm}^* - RE_{sm}^u]}{[RE_{sm}^u]}, i = 1, 2, \dots, N \quad (15)$$

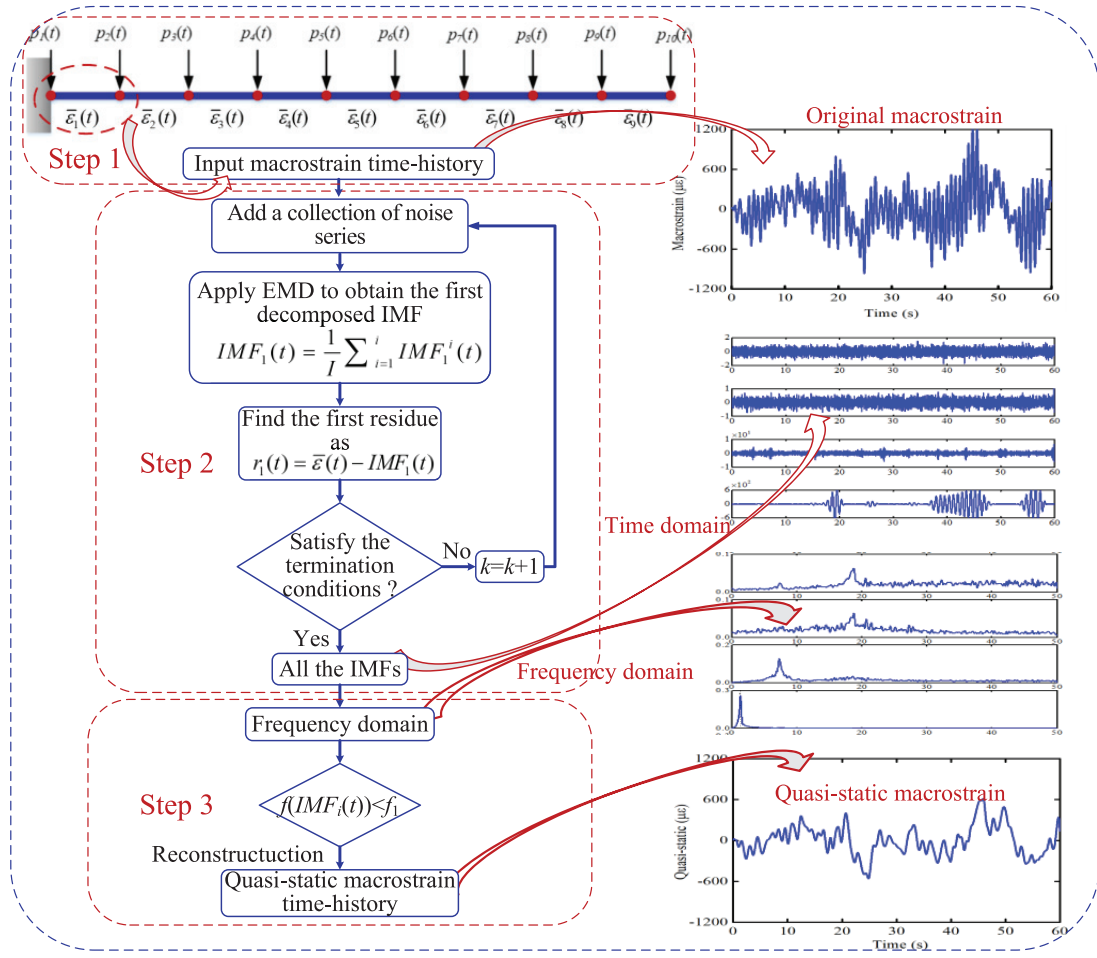


Figure 4. The main procedure for extracting quasi-static macrostrain.

where the superscript $*$ and u represent the unknown state and undamaged state, respectively. It can be found from equations (2) and (4) that damage results in a decrease of flexural stiffness at the place where it happens, the static strain response at a damaged location is larger than that at undamaged locations (Seyedpoor and Yazdanpanah, 2014). That is, if the m th element is damaged, the relative ratio RE_{sm}^* will be larger than that in intact condition, and the index β_m will be greater than zero. The damage index vector is represented as

$$\boldsymbol{\beta} = [\beta_1, \beta_2, \dots, \beta_i, \dots, \beta_N] \quad i = 1, 2, \dots, N \quad (16)$$

Thus, the positive indexes indicate potentially damaged elements. This vector gives a useful indicator for the damages, showing not only the existence of the damages but their locations as well.

3. Numerical investigation

3.1. Description of damage cases

To show the capabilities of the proposed method for structural damage detection, a cantilever beam with five damage cases are considered and investigated. Figure 5 shows the beam has the span $L = 1800$ mm and the

rectangular cross-section with the width $b = 80$ mm and depth $h = 5$ mm. The elasticity modulus is $E = 206$ GPa and the mass density is $\rho = 7800$ kg/m³. To consider the multi-damage effects, two elements are considered being damaged in this simulation. One is element 3, which is near the fix-end of the beam. The other is element 6, which is at a place far away from the fix-end. Simultaneously, both single and double damages are detected to investigate the efficiency of the proposed method. Case 1 is the intact beam, while cases 2 and 3 have a single damage incident at element 3 with 7.69% and 14.29% damage, respectively. Case 4 has double damages with 14.29% and 7.69%, respectively, at elements 3 and 6. Case 5 suffers double damages with 14.29% at elements 3 and 6, respectively. Assumed that the damage is caused by stiffness degradation, and the stiffness reduction was simulated by reducing the beam width of the elements, as shown in Figure 6. As damage occurs in the region within the gauge length, the average damage extent can be theoretically calculated by

$$\eta = \frac{EI - (EI)_{equ}}{EI} = \frac{\alpha L_2}{(1 - \alpha)(L - L_2) + L_2} \quad (17)$$

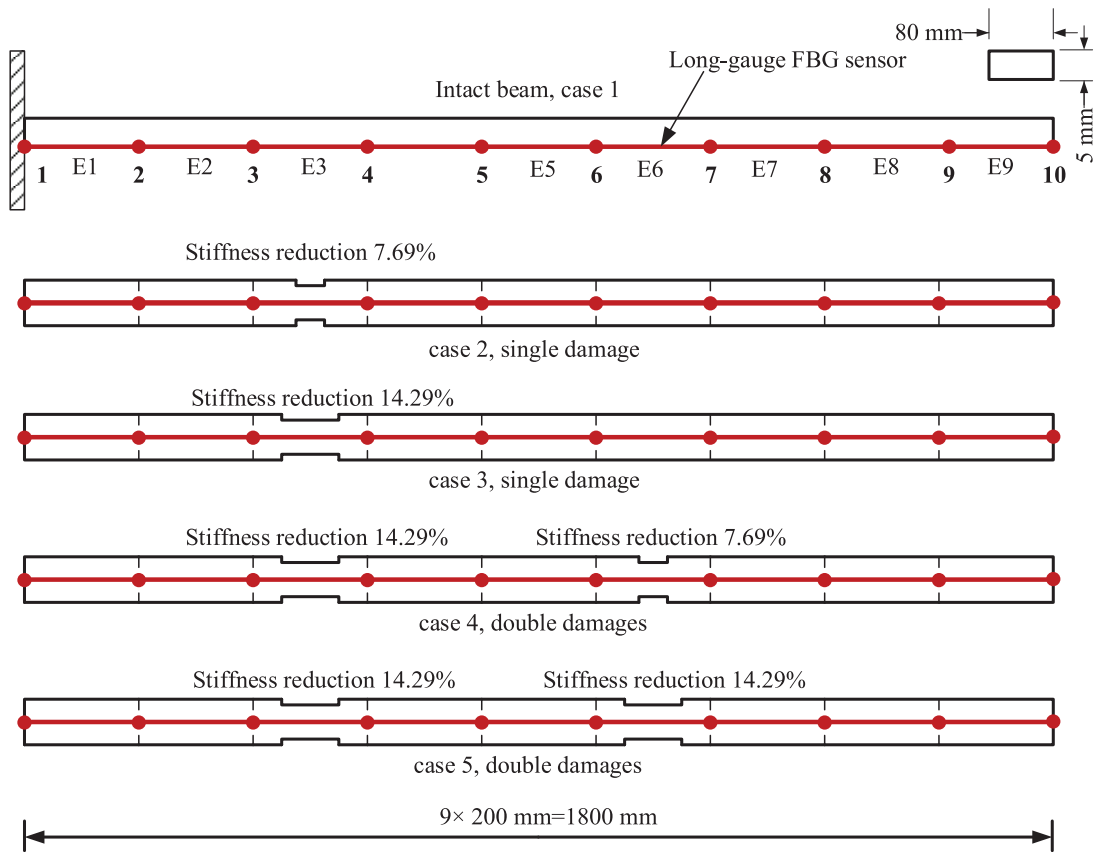


Figure 5. Details of five damage cases of the cantilever beam.

where $\alpha = (a + b)/h$. When $a = 1$ cm, $b = 1$ cm, and $L_2 = 5$ cm, the theoretical damage extent is 7.69%. For the other one, $a = 1$ cm, $b = 1$ cm, and $L_2 = 10$ cm, the damage extent is theoretically 14.29%.

Wind loads are applied as the ambient excitations to the structure, which are generated subjected to the Davenport spectrum (Davenport, 1961; Zhang et al., 2012). For brevity, Figure 7 shows the simulated 1-min fluctuating wind speed time-histories of case 1. The time step is 0.1 s, and the wind load is assumed to be the concentrated forces applied at the nodes. The responses of the cantilever beam are calculated using a time increment of 0.01 s, and the wind data are interpolated to have the same time increment, namely, with a sampling frequency of 100 Hz.

3.2. Damage detection based on quasi-static macrostrain

3.2.1. Extraction of quasi-static macrostrain. The macrostrain responses of each element along the beam were calculated and obtained by equation (5). For brevity, the measured macrostrain at element E1 of case 1 is selected as an example for presenting the quasi-static

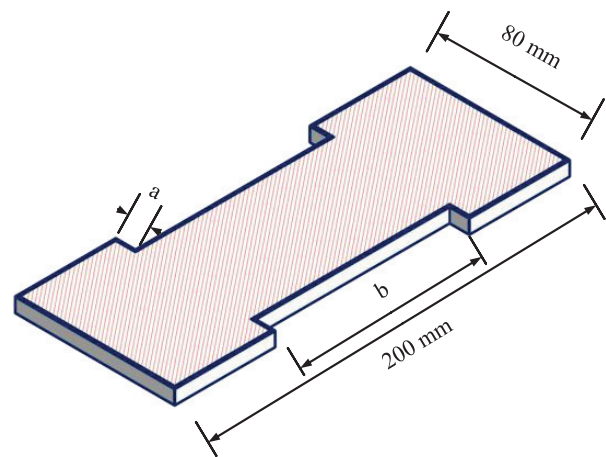


Figure 6. Details of the local damage simulation.

macrostrain extraction process using the CEEMDAN technique, in which, the standard deviation of the noise is 0.05. Figure 8 shows the results of the decomposition of the macrostrain time-history, which contains 11 components (10 IMFs and a residue). By calculating the corresponding Fourier spectrum envelope of each component, as shown in Figure 9, it can be found that the

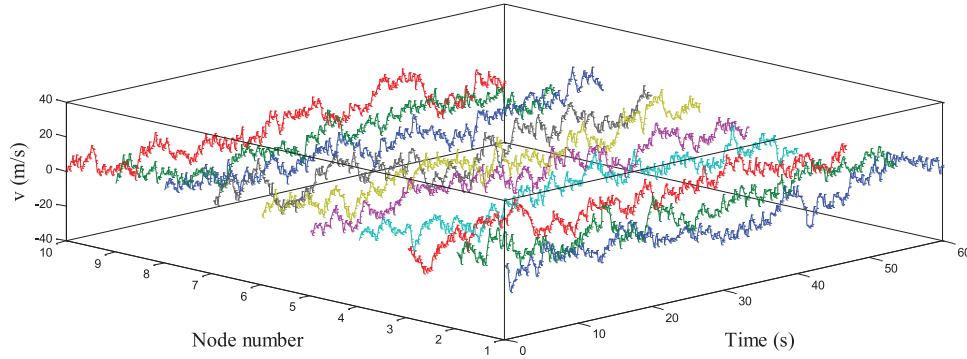


Figure 7. Time-varying wind speed of each structural node in case I.

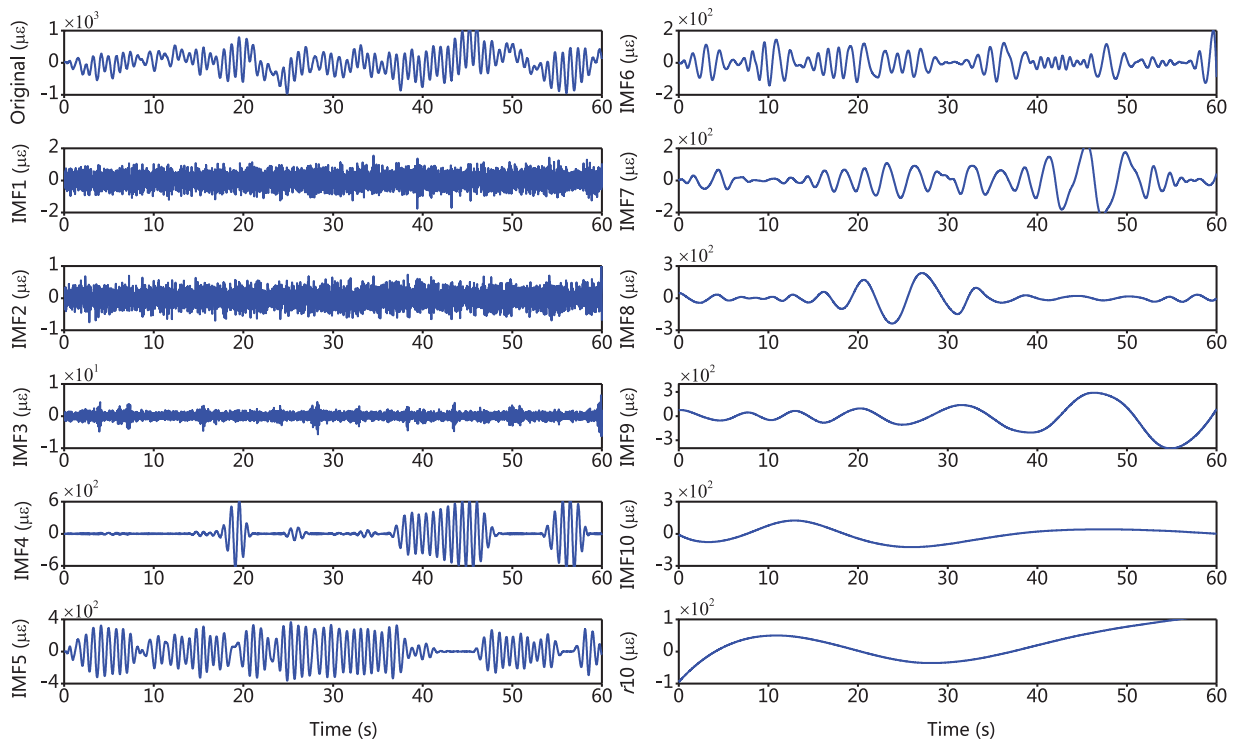


Figure 8. Decomposition results of measured macrostrain using the CEEMDAN technique.

frequencies of the IMFs decrease gradually, and the main frequency components can be judged. It can be clearly seen from these figures that the CEEMDAN has the capability to make different scale macrostrains to merge into proper IMFs, and therefore realizing the separation of dynamic and static macrostrain.

The first-order frequency of the measurement macrostrain response can be easily measured by Fourier spectrum analysis, and it is determined as 1.25 Hz. Therefore, 1.25 Hz is selected as the threshold value. Figure 9 shows the frequencies of IMF 1–IMF 5 are greater than or equal to the first-order frequency, and these IMF components should belong to the dynamic response. Correspondingly, the peak frequencies of the IMF 6–IMF 10 and the residue $r10$ are much

lower than the first-order frequency of the structure and thus belong to the low-frequency components. Thus, the composite macrostrain by adding all the low-frequency components in time-domain, named as the quasi-static macrostrain response, can be obtained.

Following the procedure of the above analysis, the quasi-static macrostrain time-histories from the macrostrain response for each damage case were extracted and are shown in Figure 10 (only the first 10 s is presented to display clearly). After that, the quasi-static macrostrain energy of each structural element in these damage cases can be calculated based on equation (12). Figure 11(a) shows the quasi-static macrostrain energy of each element in five cases. It can be seen that the decreasing trend of the quasi-static macrostrain energy

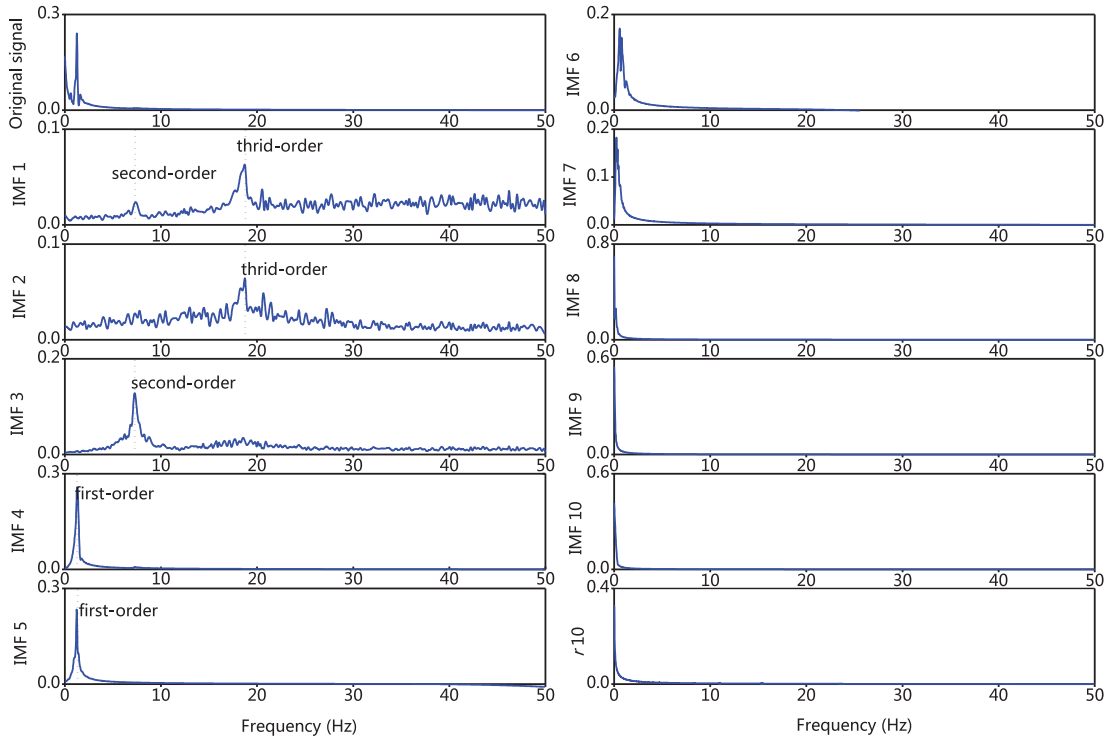


Figure 9. The IMFs in frequency-domain, from high frequency to low frequency, of measured macrostrain.

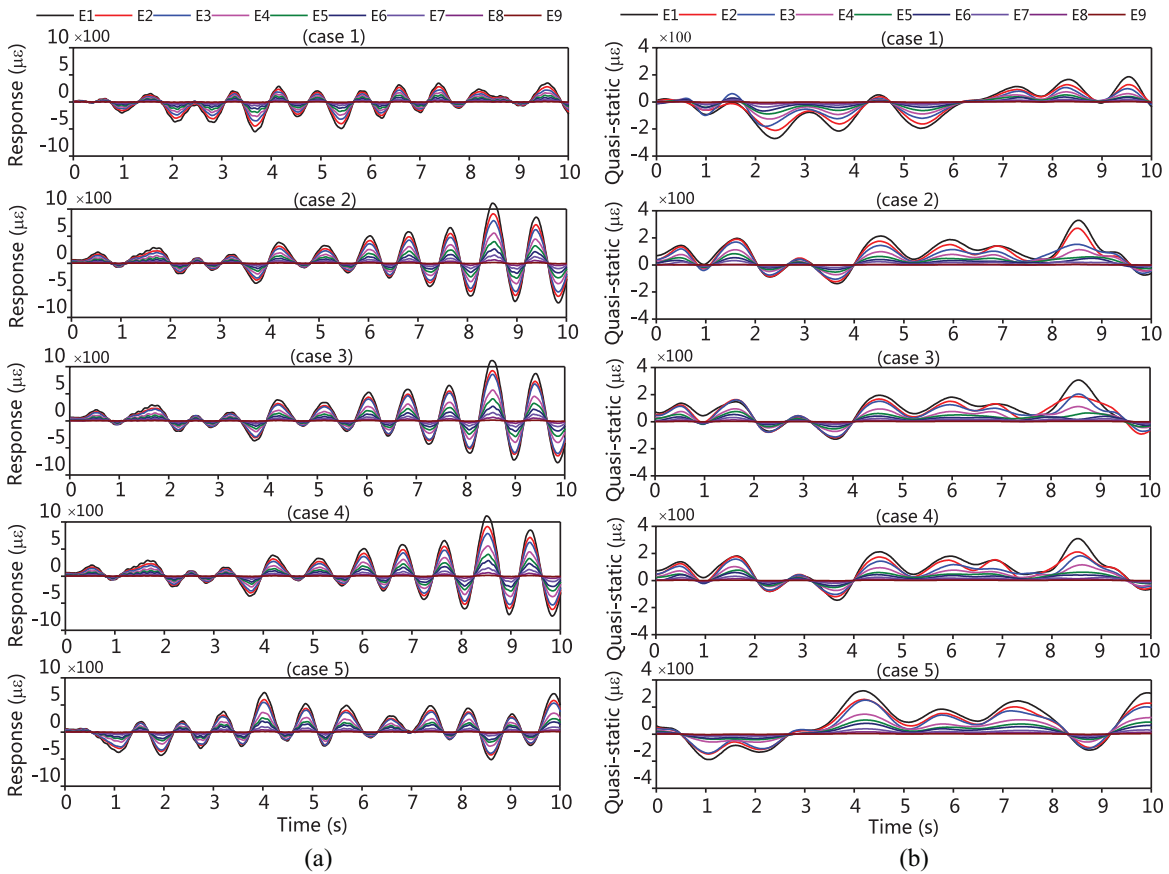


Figure 10. Extracted quasi-static strain time-histories: (a) measured macrostrain and (b) quasi-static macrostrain.

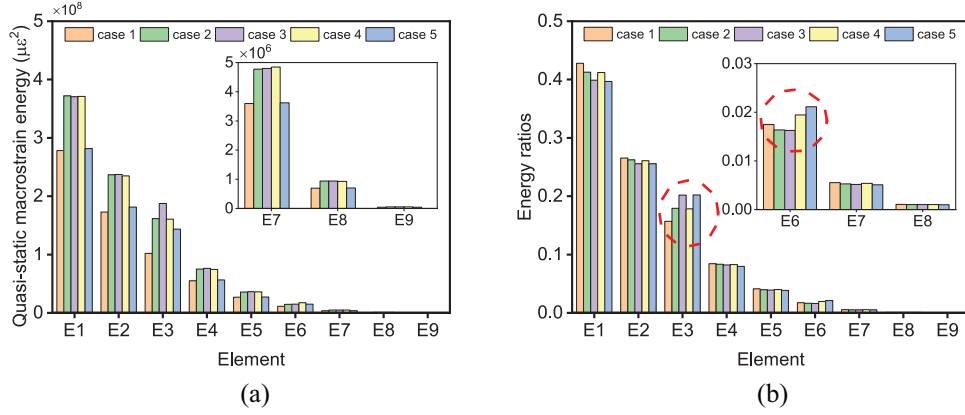


Figure 11. Quasi-static macrostrain energy and energy ratio of each element in five damage cases: (a) macrostrain energy and (b) energy ratios.

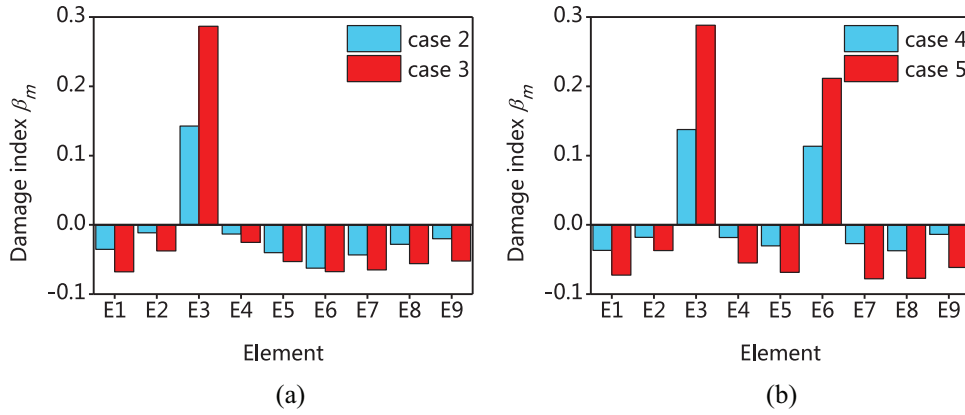


Figure 12. Damage index β_m for damage detection: (a) single damage cases and (b) double damage cases.

from the first element to the last element (fix-end to the free-end) is the same. However, different excitation results in different energy of each case, and the damage cannot be detected directly. A quasi-static energy ratio is therefore proposed to detect the local damage, which can be calculated by equation (14). Figure 11(b) shows the quasi-static energy ratios of each element in five cases. The results show the pattern of the energy ratio is similar to that of quasi-static macrostrain energy; which is also decreasing from the fix-end to the free-end. As it is expected, it could be found that the quasi-static energy ratio is much bigger when the element was damaged than that before the damage occurs. At the same time, the energy ratios of undamaged elements in damage cases are lower than those of the intact case. Thus, the difference of energy ratios between the damage and intact conditions can be a useful index to detect the local damage.

3.2.2. Damage detection. After the quasi-static macrostrains and corresponding energy ratios are acquired, the damage index, β_m , of the cantilever beam with each

damage case can be calculated. The results for five damage cases are shown in Figure 12. As was expected, the indicator can clearly show the damaged elements. Figure 12(a) shows that for case 1 and case 2, the damage index β_3 is positive for element 3 which is damaged and negative for all undamaged elements. Similarly, case 4 and case 5 in Figure 12(b) show the same phenomenon as in single damage cases, where the damage indexes are protrudent and positive for sensors deployed at the damaged elements (element 3 and element 6). Therefore, it can be concluded that the quasi-strain macrostrain-based method is a good damage detection algorithm since all damages with different damage degrees can be accurately detected and located for single and double damages.

3.3. Effect of measurement noise

Considering the measurement noises are inevitable in field measurement, it is necessary to further evaluate the robustness of the proposed method with measurement noise. As many researchers reported, it is assumed

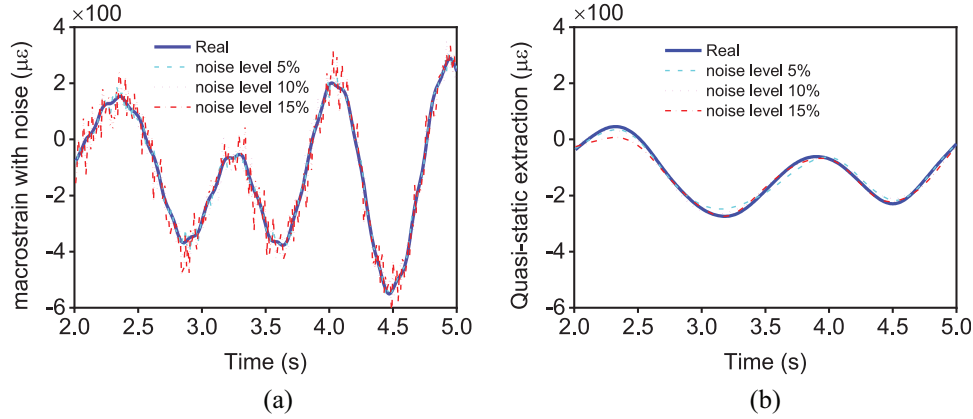


Figure 13. Macrostrain responses plus Gaussian noises and the quasi-static macrostrains: (a) macrostrain with Gaussian noise and (b) quasi-static macrostrain.

that the noise obeyed Gaussian distribution, and its rationality can be proved by the central limit theorem. Therefore, the simulated macrostrain responses are contaminated with a certain level of the Gaussian noise to generate “measured” macrostrains. Then, the macrostrain with the additive Gaussian noise can be expressed as

$$\bar{\varepsilon}_m(t) = \bar{\varepsilon}(t) + aRMS_{\bar{\varepsilon}} \cdot random \quad (18)$$

where a is the Gaussian noise level, $RMS_{\bar{\varepsilon}}$ is the root mean square value of the measured macrostrain. The variable *random* obeys the standard normal distribution $N(0, 1)$.

In this study, 5%, 10%, and 15% levels of Gaussian noise is added to the measurement macrostrain response to discuss the effects of measurement noise. Figure 13(a) shows the measurement macrostrain contaminated with noises at E1 in case 1, and the results of quasi-static macrostrains are shown in Figure 13(b). As was shown, despite the additional Gaussian noise, the quasi-static macrostrains are in good agreement with the actual one. It proves that CEEMDAN is an effective way to eliminate noise. Damage index β_m of each element in each damage case was calculated and shown in Figure 14. Even though there are some variations in the indexes which are caused by noises, but such effect is not large. Also, Figure 14(a) and (b) shows that at the damage element E3, the β_3 is much bigger than zero while the others are negative, which makes the damage index very prominent. Similar results were obtained for the double damage cases in Figure 14(c) and (d), the index of the damaged element is greater than zero, and the indexes of the undamaged elements are less than zero. Thus, all the damage locations in these damage cases can still be detected without any false indication even suffers a 15% measurement noise affects. Therefore, the detection of damage is feasible under noise conditions. The proposed damage detection

approach and the corresponding damage index are not sensitive to the measurement noise, and it is possible to detect damages for real structure.

From the above analysis, it could be found that unlike most previous approaches in distributed long-gauge FBG sensing, the proposed method in this article does not need to select reference element. Previous methods, such as MMSV-based methods (Li and Wu, 2007b; Zhou et al., 2019), the nonphysics-based approach (Kamrujjaman Serker et al., 2010), and the power spectral density (PSD)-based method (Hong et al., 2012), all requires a reference element which is usually selected at the place where is less likely to be damaged. However, it cannot be guaranteed to be always in intact status. This is particularly important when the health element can hardly to be ensured. Also, the proposed method does not require any knowledge of the structure (i.e. mode shapes, material properties, etc.) except the structural natural frequency which can be directly obtained from the measured macrostrain response. With such advantages, it can be found that the proposed method is much suitable for practical application of SHM.

4. Experimental verification

4.1. Experimental setup and macrostrain collection

To further verify the validity and performance of the proposed quasi-static macrostrain-based method for structural damage identification, experiments with a cantilever steel beam were conducted. The beam is 1.8 m long, 0.08 m wide, and 0.005 m thick. The material of the beam with a Young’s modulus of 206 GPa and a density of 7850 kg/m³. Five damage cases were also studied, both the damage locations and damage degrees are set the same with those of the simulations. To simulate the local damage more quickly and conveniently, the damage is realized by reducing the beam

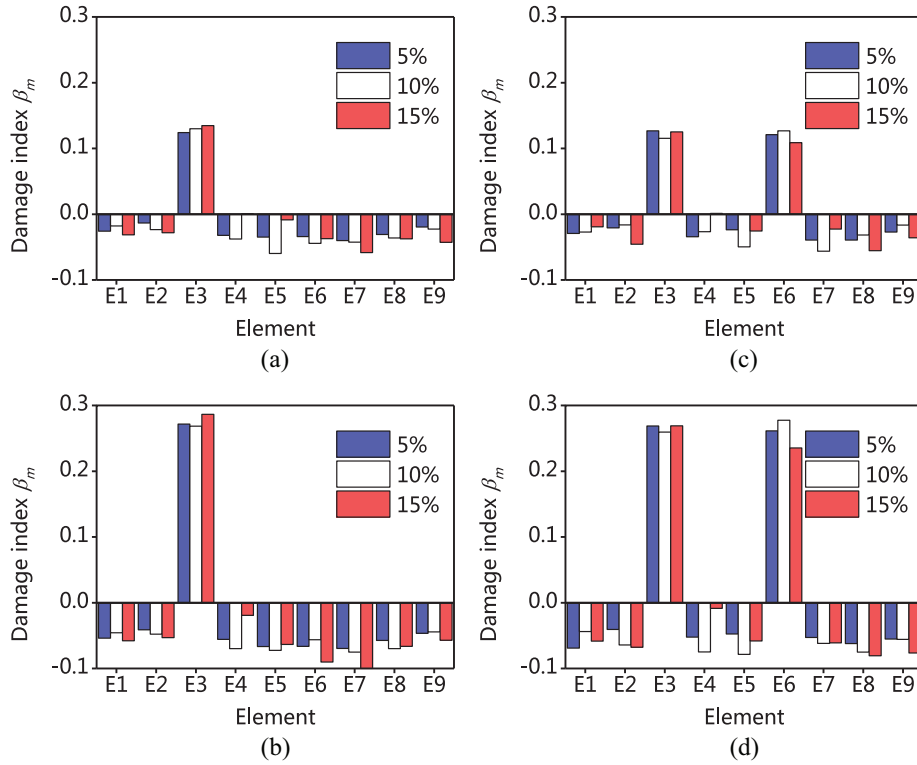


Figure 14. Damage index β_m for damage detection with various Gaussian noise levels: (a) case 2, (b) case 3, (c) case 4, and (d) case 5.

width, as is shown in Figure 15(a). Figure 15(b) shows the test specimen of damage case 5 in the lab. In this experiment, the cantilever beam is excited by a hammer with arbitrary impact forces at a random position. The developed long-gauge FBG sensor is designed to measure the averaged strain over a long-gauge length, and it can be connected in series to make a sensor network for distributed strain measurement. Based on this, the whole beam is equally divided into nine elements, and nine FBG sensors with 20 cm gauge length are pasted on the surface of the beam for macrostrain sensing. The applied FBG sensor is shown in Figure 15(c). A FBG interrogator SM 230, as shown in Figure 15(d), is used to collect the macrostrain time-histories, with the sampling rate being 500 Hz.

4.2. Damage detection

Before utilizing the CEEMDAN technique to extract the quasi-static macrostrain time histories from the long-gauge FBG sensors, the natural frequency of the beam should be confirmed to separate the dynamic components and the quasi-static components. Generally, the signal-to-noise ratio of the macrostrain response at E1 is higher than those of others for the cantilever beam. Its measured macrostrain time history and amplitude spectrum are shown in Figure 16. The results show that the first-order frequency of the beam

is 1.15 Hz. Under force excitations by the hammer, the macrostrain responses of structural elements in five damage cases were collected from the long-gauge FBG sensors for investigation. Similar to the numerical examples discussed in Section 3, quasi-static macrostrains were extracted. Figure 17 shows the measured macrostrain responses of nine elements with respect to five damage cases, as well as the corresponding quasi-static macrostrains.

When the quasi-static macrostrain time histories of each structural element were extracted for five damage cases, the macro-strain energy of each element and the corresponding energy ratio was then calculated, and the damage index vector β can be assembled afterward. Figure 18 shows the damage indexes for both single and double damage cases. Although several indexes of undamaged elements are slightly larger than zero due to the environmental disturbance, but these values are very small compared to those of the damage elements and therefore have little effects on the damage detection. Thus, it can be clearly seen that the damages, as well as their locations, can still be identified accurately in both single and double damage cases. Therefore, the results have verified that the quasi-strain macrostrain-based index is much sensitive to structural damage, and the integration of the distributed long-gauge FBG sensing technology with the proposed method is suitable for practical SHM.

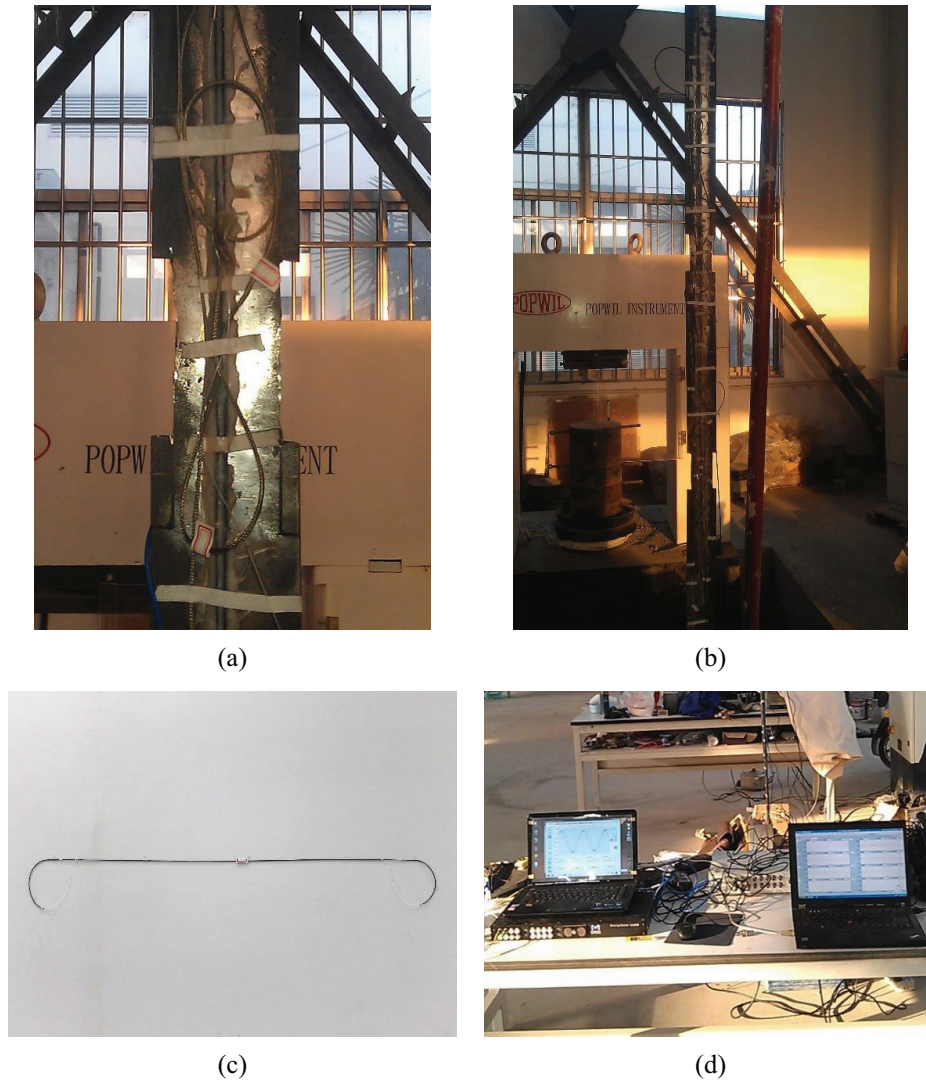


Figure 15. Components of the cantilevered steel beam experiments: (a) the realization of local damage, (b) the test sample of case 5, (c) the FBG sensor with 20 cm gauge, and (d) macrostrain collection.

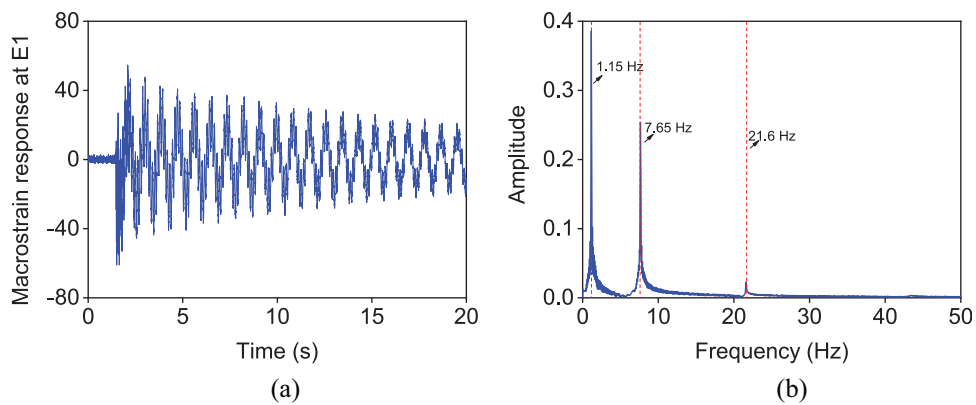


Figure 16. Measured macrostrain records for the structural vibration test: (a) macrostrain time history and (b) macrostrain amplitude spectrum.

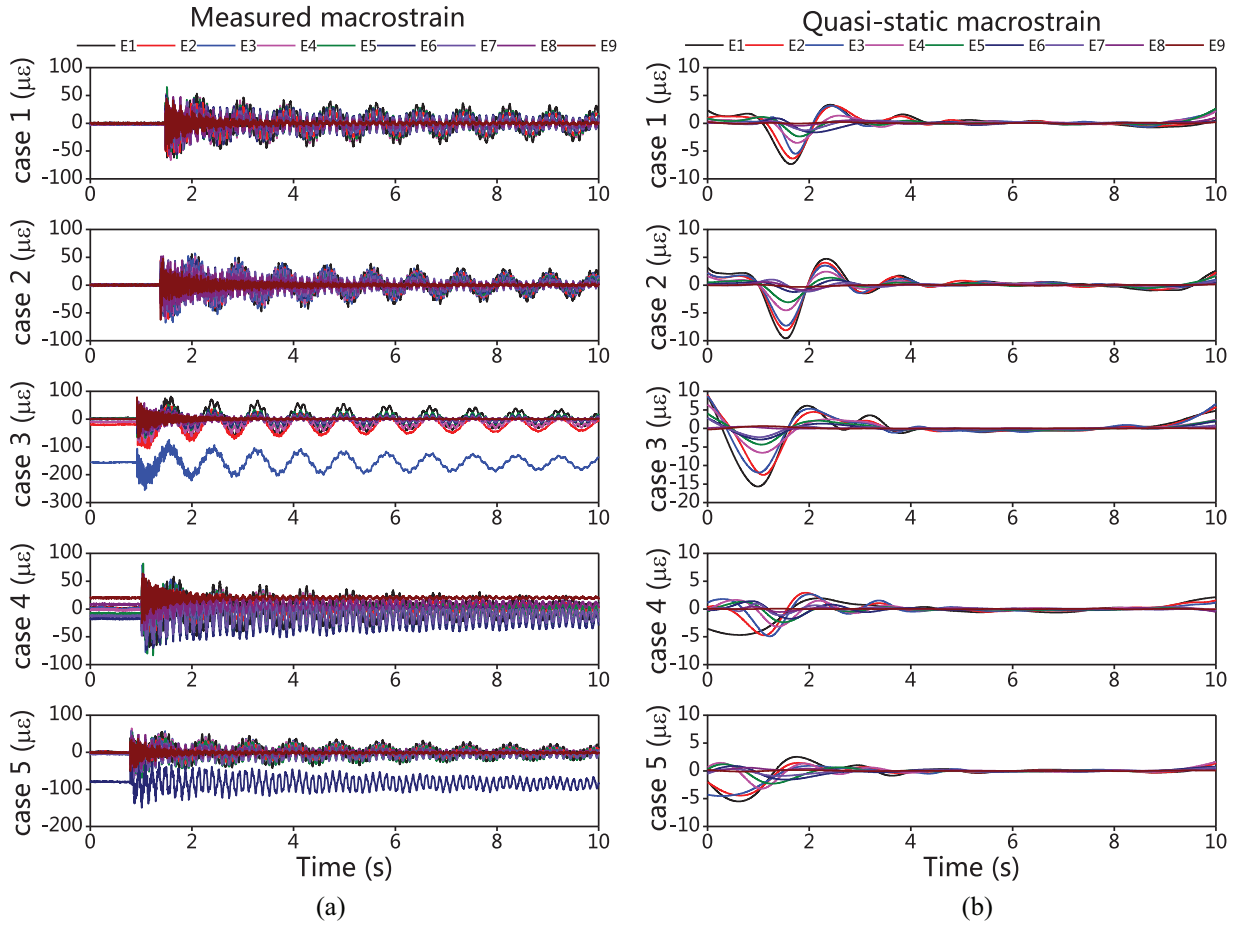


Figure 17. Extracted quasi-static macrostrain time-histories under hammer excitations: (a) measured macrostrain and (b) quasi-static macrostrain.

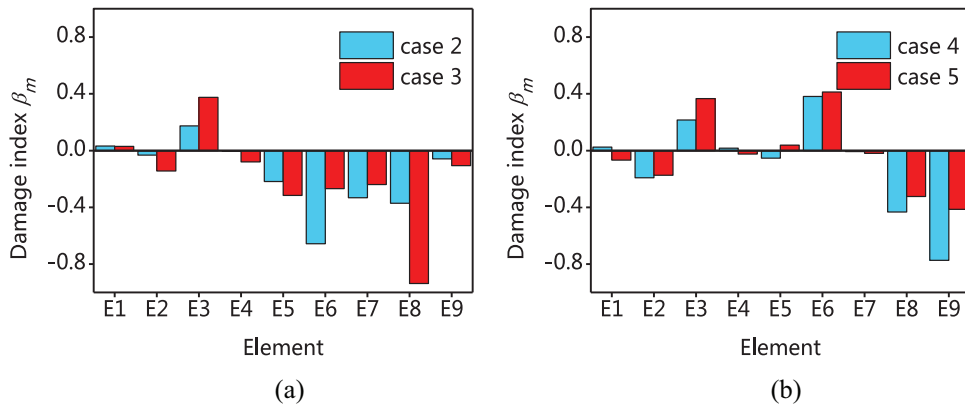


Figure 18. Damage index β_m for local damage detection under hammer excitations: (a) single damage cases and (b) double damage cases.

5. Conclusion

In this article, a quasi-static macro-strain-based damaged detection method has been proposed for detecting structural damages. The quasi-static macrostrain was obtained using the CEEMDAN technique from the

deployed distributed long-gauge FBG sensors. A quasi-static macrostrain energy ratio is then proposed to be the damage indicator. The proposed method does not require any physical modeling and reference element as other methods usually do for distributed long-gauge FBG sensor-based SHM systems. The performance of

the proposed method for structural damage detection has been verified with both numerical simulations and experiments. Five damage cases were considered and simulated, and both the single and double damages were studied. The robustness of the proposed method was further verified by considering the measurement noise. Damages were detected clearly and accurately, even under fairly high-level noises. Meanwhile, experiments were conducted at a cantilever beam. Results show that the quasi-static macrostrain-based method has high sensitivity and reliability. Thus, it has the promising potential to be applied in engineering practices for structural online health monitoring.


Declaration of conflicting interests


The author(s) declared no potential conflicts of interest with respect to the research, authorship, and/or publication of this article.

Funding

The author(s) disclosed receipt of the following financial support for the research, authorship, and/or publication of this article: The research was supported by National Key Technologies Research and Development Program of China (No. 2017YFC0805900), Innovative Venture Technology Investment Project of Hunan Province (2018GK5028), the Fund for Distinguished Young Scientists of Jiangsu Province (BK20190013), and the National Natural Science Foundation of China (Nos 51778490 and 51578140).

ORCID iDs

Zhenwei Zhou  <https://orcid.org/0000-0002-1940-2697>

Caiqian Yang  <https://orcid.org/0000-0003-2226-1618>

References

- Abdelkader R, Kaddour A, Bendiabdellah A, et al. (2018) Rolling bearing fault diagnosis based on an improved denoising method using the complete ensemble empirical mode decomposition and the optimized thresholding operation. *IEEE Sensors Journal* 18(17): 7166–7172.
- Arsenault TJ, Achuthan A, Marzocca P, et al. (2013) Development of a FBG based distributed strain sensor system for wind turbine structural health monitoring. *Smart Materials and Structures* 22(7): 075027.
- Bai LL, Han ZN, Li YF, et al. (2018) A hybrid de-noising algorithm for the gear transmission system based on CEEMDAN-PE-TFPPF. *Entropy* 20(5): 361.
- Barke D and Chiu WK (2005) Structural health monitoring in the railway industry: a review. *Structural Health Monitoring* 4(1): 81–93.
- Davenport AG (1961) The Application of statistical concepts to the wind loading of structures. *Proceedings of the Institution of Civil Engineers* 19(4): 449–472.
- Hibbeler RC (2004) *Statics and Mechanics of Materials (SI Edition)*. Singapore: Prentice Hall.
- Hong W, Cao Y and Wu ZS (2016) Strain-based damage-assessment method for bridges under moving vehicular loads using long-gauge strain sensing. *Journal of Bridge Engineering* 21(10): 04016059.
- Hong W, Wu ZS, Yang CQ, et al. (2012) Investigation on the damage identification of bridges using distributed long-gauge dynamic macrostrain response under ambient excitation. *Journal of Intelligent Material Systems and Structures* 23(1): 85–103.
- Hou ZK, Noori M and Amand RS (2000) Wavelet-based approach for structural damage detection. *Journal of Engineering Mechanics* 126(7): 677–683.
- Huang NE, Shen Z, Long SR, et al. (1998) The empirical mode decomposition and the Hilbert spectrum for non-linear and non-stationary time series analysis. *Proceedings of the Royal Society of London. Series A: Mathematical, Physical and Engineering Sciences* 454(1971): 903–995.
- Kamrujjaman Serker NHM, Wu ZS and Li SZ (2010) A nonphysics-based approach for vibration-based structural health monitoring under changing environmental conditions. *Structural Health Monitoring* 9(2): 145–158.
- Kim HS and Melhem H (2004) Damage detection of structures by wavelet analysis. *Engineering Structures* 26(3): 347–362.
- Li SZ and Wu ZS (2007a) Development of distributed long-gauge fiber optic sensing system for structural health monitoring. *Structural Health Monitoring* 6(2): 133–143.
- Li SZ and Wu ZS (2007b) A non-baseline algorithm for damage locating in flexural structures using dynamic distributed macro-strain responses. *Earthquake Engineering and Structural Dynamics* 36(9): 1109–1125.
- Ou JP and Li H (2010) Structural health monitoring in mainland China: review and future trends. *Structural Health Monitoring* 9(3): 219–231.
- Ren Y, Suganthan PN and Srikanth N (2015) A comparative study of empirical mode decomposition-based short-term wind speed forecasting methods. *IEEE Transactions on Sustainable Energy* 6(1): 236–244.
- Rippert L, Wevers M and Van Huffel S (2000) Optical and acoustic damage detection in laminated CFRP composite materials. *Composites Science and Technology* 60(14): 2713–2724.
- Rodrigues C, Félix C, Lage A, et al. (2010) Development of a long-term monitoring system based on FBG sensors applied to concrete bridges. *Engineering Structures* 32(8): 1993–2002.
- Sanayei M and Onipede O (1991) Damage assessment of structures using static test data. *AIAA Journal* 29(7): 1174–1179.
- Sanayei M and Saletnik MJ (1996) Parameter estimation of structures from static strain measurements. II: error sensitivity analysis. *Journal of Structural Engineering* 122(5): 563–572.
- Seyedpoor SM and Yazdanpanah O (2014) An efficient indicator for structural damage localization using the change of strain energy based on static noisy data. *Applied Mathematical Modelling* 38(9–10): 2661–2672.
- Torres ME, Colominas MA, Schlotthauer G, et al. (2011) A complete ensemble empirical mode decomposition with adaptive noise. In: *2011 IEEE international conference on acoustics, speech and signal processing (ICASSP)*, Prague, 22–27 May, pp. 4144–4147. New York: IEEE.
- Wang L, Liu ZW, Miao Q, et al. (2018) Complete ensemble local mean decomposition with adaptive noise and its

- application to fault diagnosis for rolling bearings. *Mechanical Systems and Signal Processing* 106: 24–39.
- Wu BT, Wu G, Lu HX, et al. (2017) Stiffness monitoring and damage assessment of bridges under moving vehicular loads using spatially-distributed optical fiber sensors. *Smart Materials and Structures* 26(3): 035058.
- Wu BT, Wu G, Yang CQ, et al. (2016) Damage identification and bearing capacity evaluation of bridges based on distributed long-gauge strain envelope line under moving vehicle loads. *Journal of Intelligent Material Systems and Structures* 27(17): 2344–2358.
- Wu ZH and Huang NE (2009) Ensemble empirical mode decomposition: a noise-assisted data analysis method. *Advances in Adaptive Data Analysis* 1(1): 1–41.
- Xu ZD, Liu M, Wu ZS, et al. (2011) Energy damage detection strategy based on strain responses for long-span bridge structures. *Journal of Bridge Engineering* 16(5): 644–652.
- Ye XW, Ni YQ and Yin JH (2013) Safety monitoring of railway tunnel construction using FBG sensing technology. *Advances in Structural Engineering* 16(8): 1401–1409.
- Zhang J, Guo SL, Wu ZS, et al. (2015) Structural identification and damage detection through long-gauge strain measurements. *Engineering Structures* 99: 173–183.
- Zhang T, Xia H and Guo WW (2012) Simulation of bridge stochastic wind field using multi-variate Auto-Regressive model. *Journal of Central South University of Science and Technology* 43(3): 1114–1121.
- Zhang WY, Qu ZX, Zhang KQ, et al. (2017) A combined model based on CEEMDAN and modified flower pollination algorithm for wind speed forecasting. *Energy Conversion and Management* 136: 439–451.
- Zhou ZW, Wan CF, Wen B, et al. (2019) Structural damage detection with distributed long-gauge FBG sensors under multi-point excitations. *Smart Materials and Structures* 28(9): 095023.